Isolated and Coupled Superquadric Loop Antennas for Mobile Communications Applications

Michael A. Jensen and Yahya Rahmat-Samii
Department of Electrical Engineering
University of California, Los Angeles
405 Hilgard Avenue
Los Angeles, CA 90024-1594, USA
Telephone: (310) 206-3847
Fax: (310) 206-3847

ABSTRACT

This work provides an investigation of the performance of loop antennas for use in mobile communications applications. The analysis tools developed allow for high flexibility by representing the loop antenna as a superquadric curve, which includes the case of circular, elliptical, and rectangular loops. The antenna may be in an isolated environment, located above an infinite ground plane, or placed near a finite conducting plate or box. In cases where coupled loops are used, the two loops may have arbitrary relative positions and orientations. Several design examples are included to illustrate the versatility of the analysis capabilities. The performance of coupled loops arranged in a diversity scheme is also evaluated, and it is found that high diversity gain can be achieved even when the antennas are closely spaced.

INTRODUCTION

Circular and non-circular loop antennas, with shapes governed by packaging considerations, often prove to be appropriate, low-profile radiators for mobile communications devices. In some instances, new efforts to combat the effects of multipath fading without requiring increased bandwidth has motivated the use of multiple elements arranged in a diversity configuration on a single transceiver [1]. In the design of such antennas, it is important to understand the effects of loop geometry and mutual coupling on the antenna impedance, radiation characteristics, and diversity performance. This paper presents the results of two sophisticated analysis tools developed for this purpose:

(a) a Galerkin moment method algorithm for loops which are isolated or located near an infinite ground plane;
(b) a finite difference time domain (FDTD) technique for loops which are isolated or placed near finite-sized conducting objects.

ANTENNA GEOMETRY

To allow characterization of a wide variety of antenna geometries with one unified formulation, the loops are modeled as superquadric curves. This geometry is a closed loop which satisfies the equation

$$|x/a|^{\nu} + |y/b|^{\nu} = 1 \qquad (1)$$

where a and b are the semi-axes in the x and y directions respectively and ν is a "squareness parameter" which controls the variation of the loop radius of curvature. The configuration is illustrated in Fig. 1 for $\nu = 2$, 3, and 10 and an aspect ratio of $b/a = 2$. As can be seen, variation of the values of a, b, and ν allows considerable flexibility in modeling many practical antenna

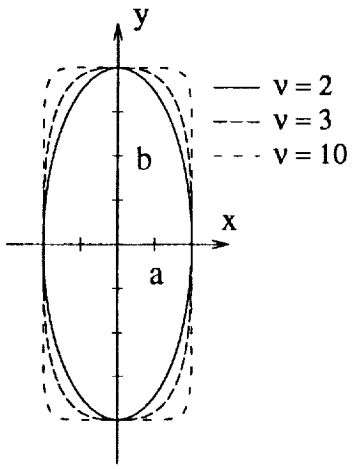

Figure 1: Superquadric geometry for $\nu = 2$, 3, and 10 with an aspect ratio of $b/a = 2$.

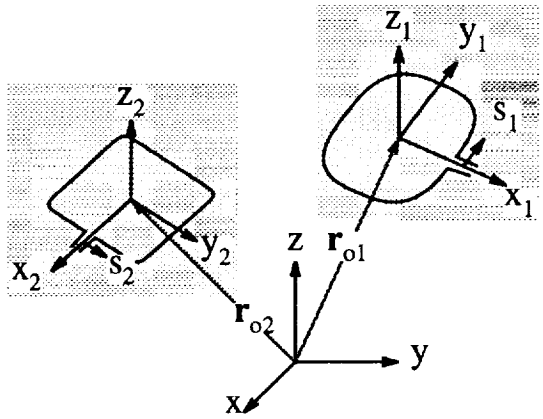

Figure 2: Geometry of two coupled loop antennas showing coordinates.

configurations. This flexibility is very important from the viewpoint of antenna packaging considerations.

For coupled loop geometries, the two superquadric antennas may have arbitrary positions and orientations and possibly different geometries, as represented in Fig. 2. Each loop is situated in its own coordinate system which may have an arbitrary position and orientation (described using Eulerian angles) with respect to the reference coordinate system.

FORMULATION

Moment Method Analysis

The moment method analysis of the coupled loop configuration makes use of a parametric expression for the superquadric curve in a coupled form of an electric field integral equation (EFIE) for thin wires. Use of this parametrization allows integration to occur on the curved loop contour rather than on the commonly-used piecewise linear representation of the curve, resulting in a more computationally efficient algorithm. Piecewise sinusoidal subsectional basis and weighting functions are used in a Galerkin form of the moment method to compute the axial current distribution along the loop. This current is then used to compute the antenna radiation pattern, directivity, and input impedance. The formulation is extended to analyze loops placed near an infinite ground plane through modification of the Green's function in the EFIE to account for the loop image. Both delta gap and magnetic frill type source models are used as excitation schemes to allow investigation of different feeding scenarios

FDTD Analysis

In order to fully evaluate the performance of loop antennas on a small box such as might be used for a hand-held radio transceiver, the effects of this conducting case must be included in the analysis. In order to investigate this configuration, the finite-difference time-domain (FDTD) algorithm is used with Yee's cubical cells and a second order absorbing boundary condition at the outer grid truncation surface. A special subcell method is used to properly account for the finite size of wires on the antenna radiation and impedance characteristics. By using properly shaped excitation functions for the antenna feed, the antenna behavior over a wide frequency

band may be determined with this time-domain formulation. An example of a design based upon these computations is provided at the end of this paper.

DIVERSITY

One of the objectives of this work is to determine the performance of the coupled superquadric loop antennas when used in a diversity scheme for a mobile communications system. In this application, we are interested in the use of space, angle, and polarization diversity to combat the effects of short-term or Rayleigh-type fading in a multipath environment. Antenna diversity scenarios in which multiple elements are used at the receiver to reduce the effects of fading are becoming more predominant as communications systems demand increased signal quality and reliability without consuming additional use of the available frequency spectrum.

A quantitative figure of merit for the performance of an antenna diversity configuration is the envelope correlation coefficient for the signals received by two different elements. In essence, this quantity provides a measure of the "similarity" of the two signals. For cases where the incident multipath field is assumed to arrive from the horizontal plane only it can be shown [1] that the envelope correlation coefficient for two antennas may be computed from the equation

$$\rho_e = \frac{\left| \int_0^{2\pi} \vec{E}_1(\pi/2,\phi) \cdot \vec{E}_2^*(\pi/2,\phi) d\phi \right|^2}{\int_0^{2\pi} |\vec{E}_1(\pi/2,\phi)|^2 d\phi \int_0^{2\pi} |\vec{E}_2(\pi/2,\phi)|^2 d\phi} \quad (2)$$

where $\vec{E}_1$ and $\vec{E}_2$ are the vector patterns associated with each of the coupled loop antennas. Generally, a value of ρ_e less than about 0.7 provides acceptable diversity returns.

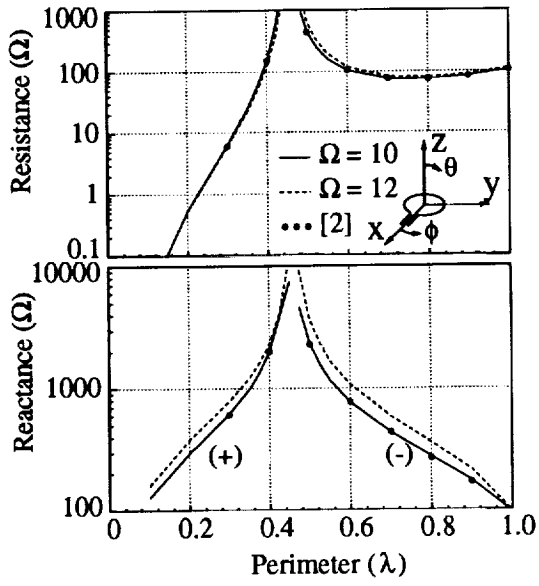

Figure 3: Input impedance versus perimeter for a single circular loop for two values of Ω. The dots are values taken from [2].

EXAMPLES

In the following examples, the parameter $\Omega = 2\ln(P/r_w)$ is used as a measure of the wire size where P is the loop perimeter and r_w is the wire radius. Fig. 3 shows the input impedance versus loop circumference for a single circular loop ($\nu = 2$, $b/a = 1$) for two values of Ω. A magnetic frill source model configured to have the dimensions of a 50Ω coaxial feeding line is used for the excitation. This plot shows that the loop antenna exhibits reasonable input impedance values for circumferences larger than about 0.7λ. The poor impedance behavior occurring for small loop circumferences can be substantially improved using proper loading techniques, thereby extending the loop to applications where the antenna size may be limited by spatial considerations. The dots in the figure correspond to data computed using a Fourier series representation for the current distribution [2]. Clearly, excellent agreement exists between the two sets of data.

An example of the use of the moment

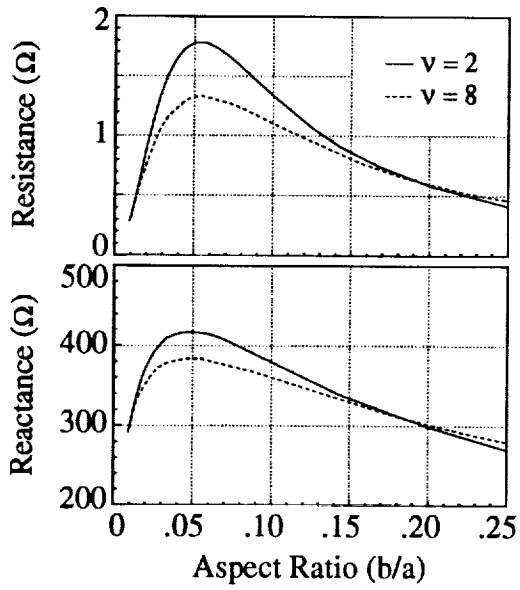

Figure 4: Input impedance versus aspect ratio b/a for a 0.25λ loop with $\Omega = 10$ for two values of ν.

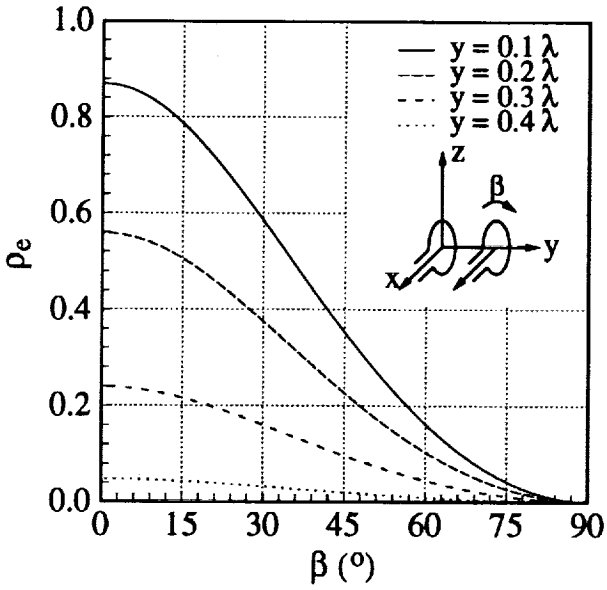

Figure 5: Envelope correlation coefficient versus rotation for 0.25λ loops ($\nu = 10$, $b/a = 1$) for various separation distances.

method to determine the effects of geometry on the loop antenna performance is illustrated in Fig. 4. This plot shows the input impedance of a 0.25λ loop with $\Omega = 10$ as the aspect ratio b/a is varied. Results are shown for $\nu = 2$ and 8. From this figure, it can be seen that the input impedance varies noticeably with loop squareness. This data can be very useful in the design of loop antennas

A key feature of loop antennas is that they may be configured to achieve high diversity performance when used in a multipath fading environment. For example, Fig. 5 illustrates the variation of the envelope correlation coefficient as a function of antenna orientation for two 0.25λ loops with $b/a = 1$ and $\nu = 10$ for several values of loop separation y. In this example, one loop is held stationary while the second is rotated about its x axis as shown in the figure inset. As can be seen from Fig. 5, low correlation coefficient values can be obtained even for small antenna spacings.

The high diversity performance of crossed loops leads to the possibility of a design such as that depicted in the inset of Fig. 6. The centroid of this antenna configuration is placed 0.2λ above an infinite ground plane to represent the scenario where the antenna is mounted on a car or other vehicle. Each loop is 0.8λ in perimeter with $\nu = 5$ and $b/a = 1$. The radiation patterns for these coupled loops normalized to the antenna directivity are shown in Fig. 6 for the principal and horizontal plane cuts. The antennas are fed 90° out of phase which results in the symmetry in the pattern in the xy plane. If proper signal combining is used with this antenna geometry, high diversity gain can be achieved.

An example of the flexibility of the FDTD methodology to predict the performance of a strip loop placed upon a hand-held transceiver case appears in Fig. 7. The geometry of the handset/antenna system is illustrated in Fig. 7(a). Fig. 7(b) demonstrates the wideband impedance behavior for this configuration At lower frequencies, the impedance varies rapidly with frequency which results in challenging matching requirements if broadband

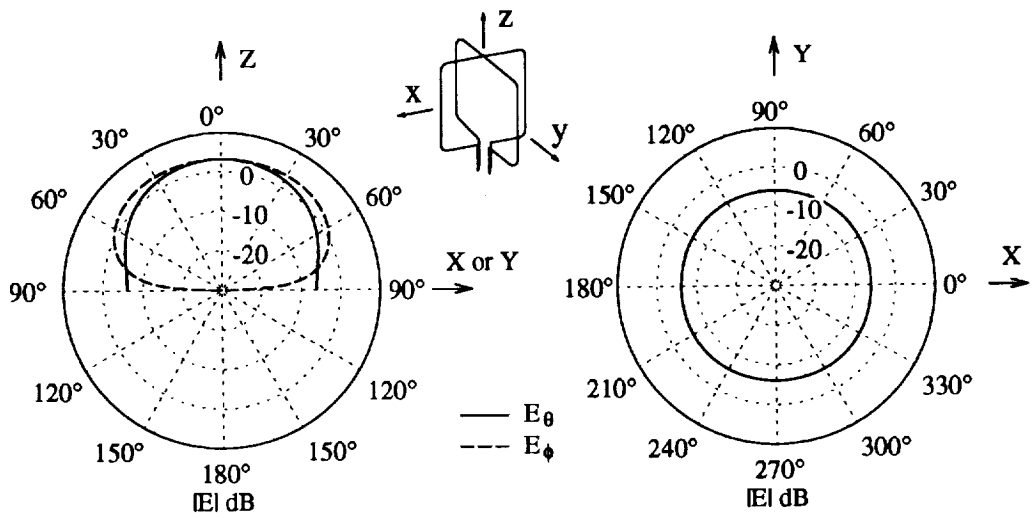

Figure 6: Directivity patterns in dB for two crossed 0.8λ superquadric loops ($\nu = 5$, $b/a = 1$) located $z_o = 0.2\lambda$ from an infinite ground plane.

performance is necessary. However, for narrowband applications, reasonable impedance values occur between the resonance peaks. For higher frequencies, the slow impedance variation with frequency allows for much wider bands of operation. The directivity patterns for the loop are provided in Fig. 7(c) for a frequency of $f = 915$MHz at which point the input impedance has a value of $53 - j246\Omega$. The asymmetries in the xz plane pattern arises from the fact that the loop is not centered on the box in the x direction to allow room for the feeding circuitry.

An example of using loading to improve the impedance characteristics of small loop antennas is provided in Fig. 8 which shows the input impedance versus frequency for a rectangular loop antenna loaded with an open circuit opposite the feed point. The loop has dimensions $a = 0.86$ cm and $b = 2.56$ cm, with a wire radius of 0.75 mm. This broadband data obtained with the FDTD methodology shows very well behaved impedance characteristics for low frequency operation, especially near 1GHz where the loop is near $\lambda/2$ in perimeter. Such an antenna may be appropriate for hand-held transceiver applications.

CONCLUSIONS

In this paper we have demonstrated the utility of newly developed computational tools based on both moment method and FDTD algorithms in the analysis of loop antennas for mobile communications applications. The analysis has been focussed on loops described by superquadric curves to allow characterization of a large number of geometries for isolated and coupled loop configurations. The diversity performance of coupled loops has been discussed and it was shown that high diversity gain is possible even for closely spaced antennas. Several key design examples were presented to illustrate the flexibility of the simulation capabilities. Naturally, these analysis tools can be applied to the characterization of numerous other possible configurations for mobile communications antennas.

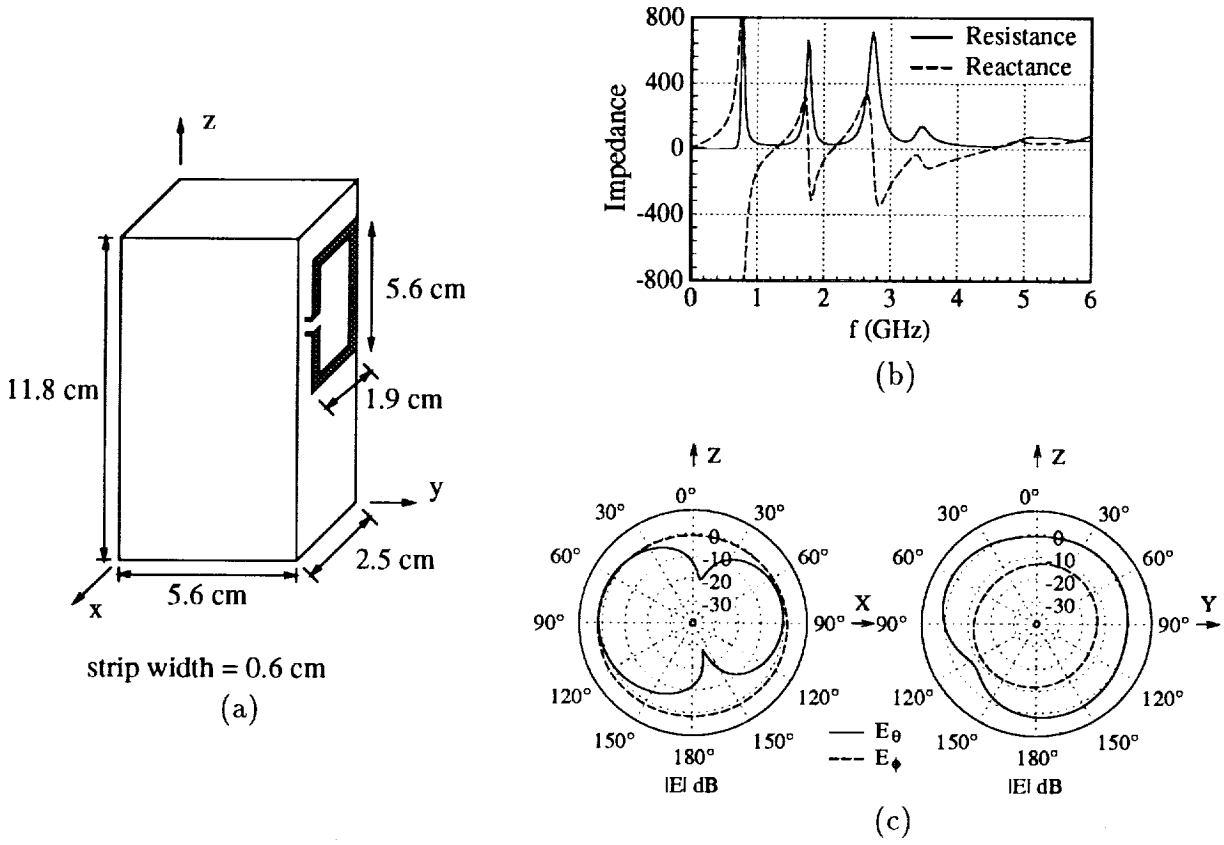

Figure 7: FDTD analysis of a strip loop on a hand-held transceiver: (a) transceiver geometry; (b) input impedance versus frequency; (c) directivity patterns at $f = 915$MHz.

Acknowledgements. This work is funded by DARPA under contract #DAAB07-92-R-C977. M. Jensen's work is also supported under a National Science Foundation Graduate Fellowship.

REFERENCES

[1] R. Vaughan and J. Andersen, "Antenna diversity in mobile communications," *IEEE Trans. Veh. Technol.*, **VT-36**, pp. 149–172, 1987.

[2] G. Zhou and G. Smith, "An accurate theoretical model for the thin-wire circular half-loop antenna," *IEEE Trans. Antennas Propag.*, **39**, pp. 1167–1177, 1991.

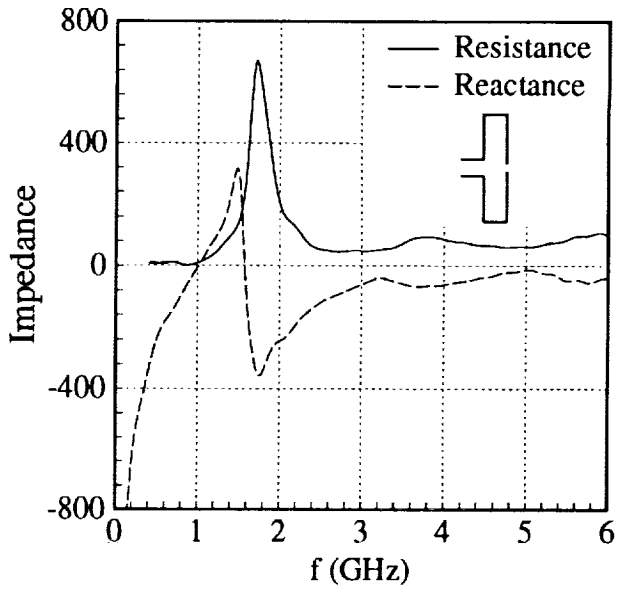

Figure 8: FDTD result of the input impedance versus frequency for a rectangular loop with $a = 0.86$ cm, $b = 2.56cm$, and $r_w = 0.75$ mm loaded with an open circuit.